

IRAS Observations of BL Lac Objects

C. Impey and G. Neugebauer

Palomar Observatory

California Institute of Technology

Pasadena, California 91125

G. Miley

Space Telescope Science Institute

Homewood Campus

Baltimore, Maryland 21218

Abstract

IRAS data has been analyzed for 35 BL Lac objects selected from a complete 5GHz radio sample, using the coadded survey database. The detection rate is 50 % with more than 40 % detected in more than one band. This compares with only 15 % of these sources that are included in the IRAS Point Source Catalog. High luminosity BL Lac objects generally have smooth energy spectra over four or five decades in frequency, consistent with incoherent synchrotron emission from 1 cm to 1 μ m. However, many low luminosity BL Lac objects have discontinuous spectra, with a large range in the spectral index at IRAS wavelengths. For BL Lacs with a total luminosity of less than 10^{44} ergs s^{-1} , most of the far infrared energy probably originates from dust heated near the galaxy nucleus. The energy budget shows that the majority of the power per unit bandwidth (νS_ν) emerges in the infrared (1 – 100 μ m).

Introduction

BL Lac objects are compact radio sources that are distinguished by their rapid variability and high linear polarization at optical and infrared wavelengths. They are among the most energetic radiators in the universe, and apparently provide the most direct and unobscured view onto the compact engine that powers many types of active galactic nuclei. A variety of evidence indicates that relativistic motion is affecting the observed properties of the most luminous BL Lac objects. For the purposes of this study, we have included highly polarized quasars, since they share with BL Lac objects the same continuum properties of a polarized, variable core.

Methods

Few extragalactic radio sources are strong enough to be included in the IRAS Point Source Catalog (PSC), and there are two ways of reaching fainter detection limits. Approximately 40 % of the mission was devoted to pointed additional observations (AOs)

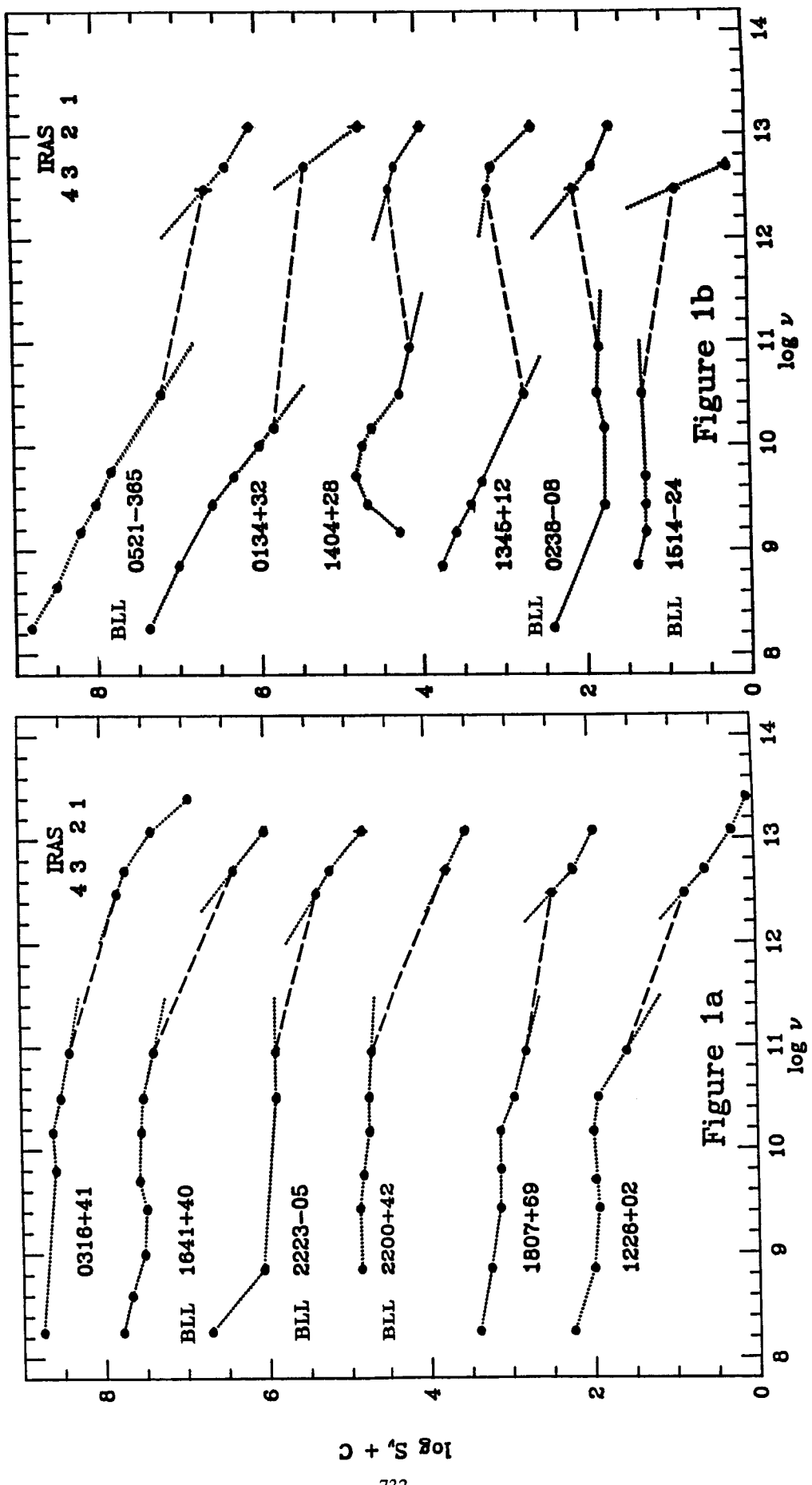
which achieved a sensitivity gain of three to eight. However, the coverage of pointed observations in this sample is very patchy. In addition, the high completeness of the survey can be traded for additional sensitivity by coadding the survey database, giving a typical sensitivity gain of a factor of three. The typical limiting sensitivities (1σ) using survey coadds are : $12 \mu\text{m} - 25 \text{ mJy}$, $25 \mu\text{m} - 35 \text{ mJy}$, $60 \mu\text{m} - 35 \text{ mJy}$, $100 \mu\text{m} - 90 \text{ mJy}$.

The absolute calibration of flux density is based on asteroids and a set of fundamental reference stars with high quality ground-based data and good photospheric models. The following bandwidths were assumed to convert instrumental fluxes to flux densities (mJy) : $12 \mu\text{m} - 13.48 \times 10^{12} \text{ Hz}$, $25 \mu\text{m} - 5.16 \times 10^{12} \text{ Hz}$, $60 \mu\text{m} - 2.58 \times 10^{12} \text{ Hz}$, $100 \mu\text{m} - 1.00 \times 10^{12} \text{ Hz}$. These factors apply to sources with energy distributions $S_\nu \propto \nu^{-1}$, for other continuum shapes a color correction has been applied. Several nonlinear correction factors have been included, along with a correction based on the positional and sampling uncertainties from the coaddition of separate flux grids. The absolute calibration is good to 2 %, 5 %, 5 % and 10 % at $12 \mu\text{m}$, $25 \mu\text{m}$, $60 \mu\text{m}$ and $100 \mu\text{m}$, but a reasonable estimate of the final uncertainty in the survey coadded fluxes is 15 %. However, many of the uncertainties in IRAS data are not normally distributed, so the contour plots and source extractions for each source have been carefully checked for anomalies, such as nearby strong sources, tracks due to bad detectors, cirrus sources at $60 \mu\text{m}$ and $100 \mu\text{m}$, unusual source shapes, poor correlation coefficients for the template flux, and large differences between the median and local signal-to-noise in the field.

The absolute accuracy of the IRAS positions, established by a grid of $\sim 10,000$ SAO stars, is 2.8 arcsec in-scan and 15.6 arcsec cross-scan. The mean differences between the IRAS positions and radio positions (accurate to 1 arcsec) for the detected sources are : $12 \mu\text{m} - 22 \text{ arcsec}$, $25 \mu\text{m} - 35 \text{ arcsec}$, $60 \mu\text{m} - 25 \text{ arcsec}$ and $100 \mu\text{m} - 58 \text{ arcsec}$. These differences are no more than a single beam width in each waveband. The surface density of point sources down to the faint limit of the detections ($\sim 35 \text{ mJy}$ at $60 \mu\text{m}$) is roughly 54 per square degree. This assumes a surface density of 0.6 sources per square degree with $S(60 \mu\text{m})/S(25 \mu\text{m}) > 1$ at a galactic latitude greater than 30° , and uses the observed Euclidean source counts of $\log N \propto 1.5 \log S$. The probability of a chance coincidence between an unassociated source and the radio source position is less than 0.01 %. Therefore, the misidentification rate in this sample of 35 will be small.

Discussion

No complete sample of BL Lac objects exists, but we can get a representative idea of the properties by studying the energy distributions of BL Lacs selected from a complete radio sample. About 40 % of a sample of strong, compact radio sources show the strong optical polarization characteristic of BL Lac objects; the rest are identified with quasars and radio galaxies. The energy distributions divide easily into two classes on the basis of the morphology of the radio/infrared energy distributions. In one set of sources the infrared emission joins smoothly onto the compact radio emission, in the sense of a smooth and monotonic change of the spectral index α , where $\alpha = \text{dlog } S_\nu / \text{dlog } \nu$. These sources generally include the high luminosity BL Lac objects or blazars (Figure 1a). The other



group of sources show a discontinuity between the radio and infrared emission, in the sense that the (generally steep spectrum) radio emission projects to a flux density well below the level of the IRAS data. Therefore, the spectral index must change sign at submillimeter wavelengths. These sources generally include the low luminosity BL Lac objects embedded in nearby elliptical galaxies (Figure 1b). The radio energy distributions in Figures 1a and 1b are taken from Kuhr *et al* (1981) or Owen *et al* (1980), with the IRAS data plotted on the high frequency side of the figure. The comparison of nonsimultaneous radio and infrared data does not prevent a discussion of the average spectral shape of a collection of sources. Note that the IRAS data almost fills in the spectrum from 10^8 Hz to 10^{14} Hz.

The spectral energy distribution alone cannot pin down the emission mechanism for the infrared energy in BL Lac objects. The sources in Figure 1a have smooth continuous spectra between radio and infrared wavelengths, indicating a single emission process operating. These sources also show variability at both millimeter and near infrared wavelengths, and often linear polarization which points unambiguously to the synchrotron process. Some conclusions can be drawn about the synchrotron process in these high luminosity BL Lac objects. Two useful parameters can be calculated. One is the spectral index in the range $10 - 100 \mu\text{m}$, and the mean and rms dispersion of this slope for the luminous BL Lacs is $\alpha_{\text{IR}} = 1.02 \pm 0.19$. This is close to the canonical mean slope that has long been quoted both for quasars (Neugebauer *et al* 1979) and BL Lac objects (Cruz-Gonzales and Huchra 1984), but the dispersion is surprisingly small. For example, the range of infrared slope for the low luminosity radio galaxies is very large, $\alpha_{\text{IR}} = 1.74 \pm 0.81$. In addition, the optical spectral indices of a similar set of radio strong quasars (Neugebauer *et al* 1979) give a value $\alpha_{\text{opt}} = 1.89 \pm 0.79$, a steeper slope with much larger scatter. Second, the wavelength at which the spectrum turns down can be calculated. In the synchrotron model this would be associated with the most compact synchrotron component becoming optically thin. In some cases the energy spectra show a smooth and continuous curvature, and a polynomial or parabolic functional form is equally valid in fitting the spectra. In addition, there is a small scatter in the distribution of ν_B , the break frequency which has a mean and dispersion of $\log \nu_B = 11.73 \pm 0.71$. Therefore, there is a homogeneity in the synchrotron spectra of objects with a wide range of apparent luminosity (relativistic motion in some of these sources may reduce the range of intrinsic luminosity). Since energy loss mechanisms act to steepen the spectrum at high energies in the ultraviolet, there will be a larger scatter in the optical and UV spectral indices (some of this increased scatter is also due to the contribution of the broad UV *bump* seen in many quasars). However, at IRAS wavelengths the uniformity in α_{IR} must reflect a uniformity in the energy spectrum of the accelerated electrons. Similarly, the narrow dispersion in ν_B may reflect a uniformity in the physical conditions in the synchrotron core. Note that variability or errors in the extrapolation used to determine ν_B will increase rather than decrease the scatter. From basic synchrotron theory, even a monoenergetic electron distribution will integrate into a spectral energy distribution with a width of $3/2$ decades in ν/ν_c where $\nu_c \sim \gamma^2 B$ is the critical frequency where most of the synchrotron power emerges. Therefore, any feature such as a turnover or kink in an electron energy spectrum will integrate into a feature at least as broad as the rms of ν_B for the luminous BL Lacs. On the other hand, if ν_B is

regulated by the opacity of the source, then this result may point to a narrow range in the value of the equipartition magnetic field in the cores of sources of very different luminosity.

The high luminosity BL Lacs have bolometric luminosities in the range $10^{45} - 10^{48}$ ergs s $^{-1}$, and 20 – 30 % of the luminosity is emitted in the infrared. For the low redshift BL Lacs, the energy spectra (Figure 1b) indicate a component with half power width of three decades of frequency and a peak in the range 100 μm to 1 mm. The lack of a smooth interface between the radio and infrared data is not due to variability, since these radio galaxies mostly have steep radio spectra with a small fraction of the flux in a compact variable core. Therefore it is likely that dust in the nucleus of the host galaxy is reradiating the moderate infrared power ($L_{\text{IR}} \sim 10^{43} - 10^{44}$ ergs s $^{-1}$) seen at IRAS wavelengths. Because of the steep infrared slope and inversion at millimeter wavelengths, a high fraction of 40 – 60 % of the radio galaxy luminosity can emerge in the infrared. The weaker correlation between radio and infrared power in radio galaxies does not rule out the existence of some galaxies where nonthermal radiation dominates at IRAS wavelengths. For instance, Heckman *et al* (1983) and Elvis *et al* (1984) have shown that radio galaxies with broad emission lines tend to have nonthermal power laws in the 1 – 20 μm . In general, there may be both thermal and nonthermal components in the infrared emission, and the energy distribution alone is insufficient to disentangle them. For example, in NGC 1052 the lack of 10 μm variability and steep infrared power law indicate a strong thermal component (Becklin *et al* 1982), while the significant 2 μm linear polarization means that there is also an embedded synchrotron source (Rieke *et al* 1982). For BL Lacs with $L_{\text{IR}} < 10^{44}$ ergs s $^{-1}$, the relative contributions of thermal and nonthermal radiation must be decided on an individual basis.

Acknowledgments

The extensive efforts of Helen Hanson in generating and analyzing the survey coadds is gratefully acknowledged. We thank Walter Rice, Carol Persson and Gene Kopan at IPAC for constant help and encouragement. This work was carried out under NASA/IRAS grant 97582 administered through Caltech/JPL. CDI received support from a Weingart Fellowship.

References

- Becklin, E.E., Tokunaga, A.T. and Wynn-Williams, C.G. 1982, *Ap.J.*, **263**, 624.
- Cruz-Gonzales, I. and Huchra, J.P. 1984, *A.J.*, **89**, 441.
- Elvis, M., Willner, S., Fabbiano, G., Carleton, N., Lawrence, A. and Ward, M. 1984, *Ap.J.*, **280**, 574.
- Heckman, T.M., Lebofsky, M.J., Rieke, G.H. and van Breugel, W. 1983, *Ap.J.*, **272**, 400.
- Kuhr, H., Witzel, A., Pauliny-Toth, I.I.K. and Nauber, U. 1981, *Astron.Ap.Supp.*, **45**, 367.
- Neugebauer, G., Oke, J.B., Becklin, E.E. and Matthews, K. 1979, *Ap.J.*, **230**, 79.
- Owen, F.N., Spangler, S.R. and Cotton, W.D. 1980, *A.J.*, **85**, 351.
- Rieke, G.H., Lebofsky, M.J. and Kemp, J.C. 1982, *Ap.J.Lett.*, **252**, L53.